

HAtt-Flow: Hierarchical Attention-Flow Mechanism for Group Activity Scene Graph Generation in Videos

Naga VS Raviteja Chappa¹, Pha Nguyen¹, Thi Hoang Ngan Le¹, Khoa Luu¹

¹University of Arkansas

{nchappa, panguyen, thile, khoaluu}@uark.edu,

arXiv:2312.07740v1 [cs.CV] 28 Nov 2023



Figure 1. A sample video from our Group Activity Scene Graph (GASG) Dataset. The top row displays keyframes featuring overlaid bounding boxes, each annotated with a unique ID for consistency. Below, the timeline tubes provide a comprehensive temporal representation of scene graph annotations for distinct attributes, including *Appearance*, *Interaction*, *Position*, *Relationship*, and *Situation*. These annotations offer nuanced details, enhancing scene understanding and contributing to a more refined video content analysis. **Best viewed in color and zoomed.**

Abstract

Group Activity Scene Graph (GASG) generation is a challenging task in computer vision, aiming to anticipate and describe relationships between subjects and objects in video sequences. Traditional Video Scene Graph Generation (VidSGG) methods focus on retrospective analysis, limiting their predictive capabilities. To enrich the scene understanding capabilities, we introduced a GASG dataset extending the JRDB dataset with nuanced annotations involving Appearance, Interaction, Position, Relationship, and Situation attributes. This work also introduces an innovative

approach, *Hierarchical Attention-Flow (HAtt-Flow) Mechanism*, rooted in flow network theory to enhance GASG performance. Flow-Attention incorporates flow conservation principles, fostering competition for sources and allocation for sinks, effectively preventing the generation of trivial attention. Our proposed approach offers a unique perspective on attention mechanisms, where conventional "values" and "keys" are transformed into sources and sinks, respectively, creating a novel framework for attention-based models. Through extensive experiments, we demonstrate the effectiveness of our HAtt-Flow model and the superiority of our proposed Flow-Attention mechanism. This work repre-

sents a significant advancement in predictive video scene understanding, providing valuable insights and techniques for applications that require real-time relationship prediction in video data.

1. Introduction

Visual scene understanding is a foundational challenge in computer vision, encompassing the interpretation of complex scenes, objects, and their relationships within images and videos. This task is particularly intricate in video, where temporal dynamics and multi-modal information introduce unique complexities. Group Activity Video Scene Graph (GAVSG) generation, which involves predicting relationships between objects in a video across multiple frames, stands at the forefront of this endeavor.

In recent years, significant progress has been made in video understanding. Techniques such as Video Scene Graph Generation (VidSGG) have allowed us to extract high-level semantic representations from video content. However, VidSGG typically operates in a static, retrospective manner, constraining its predictive capabilities. The GAVSG dataset, on the other hand, extends the scope of visual scene understanding to anticipate and describe subject and object relationships and their temporal evolution.

In the closely-linked domain of human-object interaction (HOI)[17], transferable techniques have proven effective for scene graph generation (SGG) tasks [7, 13, 15, 19, 20, 25, 27, 35, 36, 39, 49, 56–58, 70, 71, 75], some of which inspired the foundation of PSG dataset baselines [28, 76].

In the context of SGG, diverse methodologies have been explored, from probabilistic graphical models and AND-OR grammar approaches [1–4, 30, 31, 46, 59] to knowledge graph embeddings like VTransE [72] and UVTransE [21]. Recent endeavors delve into challenges such as the long-tailed distribution of predicates [11, 53], visually-irrelevant predicates [37], and precise bounding box localization [26]. As shown in the Fig. 2, we can observe that the previous methods can detect the subjects and objects in the scene. However, they need to generate a well-defined scene graph, whereas our method can learn all the nuanced relationships among the subjects and objects in the scene to produce a fine scene graph.

To address the limitation of enriched-learning of the group activities in the scene, we introduced the GASG dataset which includes nuanced annotations in the form of five different attributes. This can help to set a better scene graph generation benchmark than the existing datasets in this domain. In this work, we propose a novel approach for GAVSG that draws inspiration from flow network theory, introducing Flow-Attention. This mechanism leverages flow conservation principles in both source and sink aspects, introducing a competitive mechanism for sources and an allocation mech-

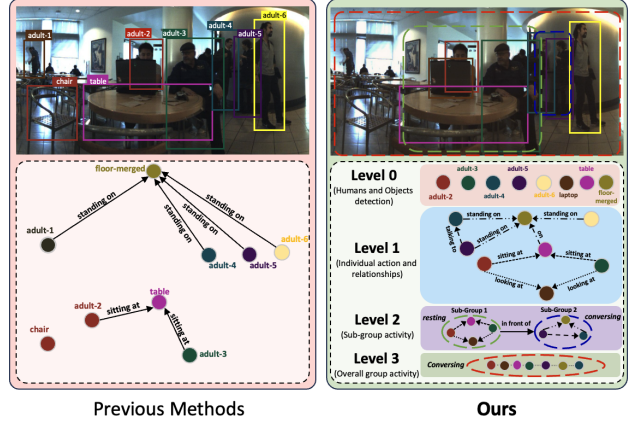


Figure 2. Comparison of HAtt-Flow result with other Scene Graph Generation methods. **Best viewed in color and zoomed.**

Table 1. Comparison of existing datasets. **GA** is the group activity label, **H-H**, **H-O** and **O-O** represents interaction between *Human and Human*, *Human and Object* & *Object and Object*.

Datasets	Settings	Annotations			Attributes		
		BBox	IDs	GA	H-H	H-O	O-O
ActivityNet [6]	1	✓	✗	✗	✗	✓	✗
MSRVTT [61]	1	✓	✗	✗	✗	✓	✗
MSVD [42]	1	✓	✗	✗	✗	✓	✓
PSG [64]	1	✓	✓	✗	✓	✓	✓
PVSG [65]	1	✓	✓	✗	✓	✓	✓
GASG (Ours)	5	✓	✓	✓	✓	✓	✓

anism for sinks. This innovative approach mitigates the generation of trivial attention and enhances the predictive power of GAVSG. We build upon a new perspective on attention mechanisms, rooted in flow network theory, to design our GAVSG framework. The conventional attention mechanism aggregates information from “values” and “keys” based on the similarity between “queries.” By framing attention in terms of flow networks, we transform values into sources and keys into endpoints, thus creating a fresh perspective on the attention mechanism.

Contributions: The main contributions of our work are three folds. First, we introduce a novel dataset¹ with nuanced attributes that aid the scene graph generation task in the group activity setting. Second, our work advances the state of the art in predictive video scene understanding by introducing Flow-Attention and redefining attention mechanisms by incorporating hierarchy awareness. Third, we demonstrate the effectiveness of our approach through extensive experiments and achieve State-of-the-Art performance over the existing approaches.

¹The dataset is available for verification in the supplementary material.

2. Related Work

Group Action Recognition (GAR). Group Action Recognition (GAR) has witnessed a shift towards deep learning methodologies, notably convolutional neural networks (CNN) and recurrent neural networks (RNN)[5, 10, 22, 23, 32, 43, 47, 55, 62]. Attention-based models and graph convolution networks are crucial in capturing spatial-temporal relations in group activities. Transformer-based encoders, often coupled with diverse backbone networks, excel in extracting features for discerning actor interactions in multimodal data[14]. Recent innovations, such as MAC-Loss, introduce dual spatial and temporal transformers for enhanced actor interaction learning [18]. The field continues to evolve with heuristic-free approaches like those by Tamura et al., simplifying the process of social group activity recognition and member identification [50].

Scene Graph Generation (SGG). In Scene Graph Generation (SGG), the traditional two-stage paradigm involves object detection and pairwise predicate estimation [8, 9, 24, 29, 34, 38, 44, 51, 60, 63, 69, 73]. Recent advancements include knowledge graph embeddings, graph-based architectures, energy-based models, and linguistic supervision [16, 40, 48, 51, 66–68, 74]. To address challenges like long-tailed distribution and visually irrelevant predicates, the field has seen a pivot towards panoptic segmentation-based SGG, inspired by the simultaneous generation of scene graphs and semantic segmentation masks [26]. Notably, insights from the closely-linked domain of human-object interaction (HOI) have influenced SGG techniques [7, 13, 15, 19, 20, 25, 27, 35, 36, 39, 49, 56–58, 70, 71, 75].

Video Scene Graph Generation (VidSGG). VidSGG, initiated by Shang *et al.* [45], explores spatio-temporal relations in videos. Research has delved into spatio-temporal conditional bias, domain shift between image and video scene graphs, and embodied semantic approaches using intelligent agents. Notable methods include TRACE [54], which separates relation prediction and context modeling, and Embodied Semantic SGG, employing reinforcement learning for path generation by intelligent agents [12, 33]. Yang *et al.* [65] proposed a transformer encoder based baseline model to evaluate their proposed panoptic video scene graph dataset which includes fusing the extracted features of the subjects in the scene.

2.1. Limitation of Prior Datasets

We presented a detailed comparison of existing datasets in Tab. 1. The limitations of prior datasets become particularly conspicuous when we contemplate the intricate nature of group activity within the visual content. Most of these datasets have predominantly concentrated on specific individual action types, often neglecting the complex nature of group activities in real-world interactions. This constrained focus has created obstacles in developing models capable of

addressing a wide range of action classifications, limiting their adaptability to diverse real-world scenarios. Furthermore, earlier datasets often underscore relationships within isolated fragments of the relational graph, occasionally omitting the complexities of more extensive and intricate scenes. Some of these datasets have suffered from sparse annotations, which, at times, have led to a lack of comprehensive relationship modeling and potential model bias.

Notably, there remains to be a significant void in the representation of scenes featuring dense crowds of people. These settings bring about formidable challenges related to occlusion management and a nuanced understanding of complex interactions within such contexts.

In response to these limitations, we introduce *Group Activity Scene Graph (GASG)* dataset that directly addresses these issues. The dataset boasts various scenes and settings (which are represented as attributes in the annotations), spanning distinct scenarios, effectively differentiating it from the prior datasets. It excels in capturing five critical features in group activity: appearance, situation, position, interaction, and relations. Furthermore, this dataset comprehensively tracks the movements and interactions of individuals and sub-groups, allowing for a profound understanding of their dynamics and activities over time. With a rich dataset on these aspects, this GASG dataset lays the groundwork for a new paradigm in understanding complex group activities within scenarios characterized by dense populations, thereby pushing the boundaries of group activity recognition.

3. Dataset Overview

3.1. Data Collection and Annotation

This GASG dataset comprises a rich collection of videos from the JRDB dataset, offering a unique perspective on sub-group and overall group activities. This dataset provides comprehensive coverage of various activities and introduces essential tracking information.

The tracking information within the GASG dataset facilitates a detailed understanding of individuals and sub-groups within each frame. This information includes the trajectory, position, and interactions of each actor. The dataset defines five key aspects for comprehensive scene understanding:

- *Interaction:* This aspect characterizes the dynamic interactions between subjects and objects, shedding light on how individuals and sub-groups engage with each other.
- *Position:* The dataset includes precise data on the location and orientation of subjects and objects, enhancing the analysis of their spatial relationships during activities.
- *Appearance:* Visual traits of subjects and objects are meticulously captured, allowing for detailed examinations of their attributes and characteristics.
- *Relationship:* Understanding the associations and connections between subjects and objects is essential for decipher-

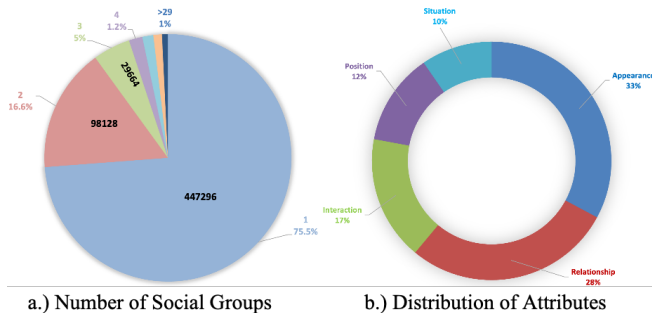


Figure 3. Statistics of the GASG dataset, number of social groups, and the attributes in the dataset. **Best viewed in color and zoomed.**

ing the complex interplay within group activities. This aspect provides insight into the underlying dynamics of relationships within the scenes.

- **Situation:** To provide environmental context, the GASG dataset offers descriptors highlighting the contextual information surrounding subjects and objects, enabling researchers to consider the broader setting in their analyses. These five key aspects—Interaction, Position, Appearance, Relationship, and Situation—form the backbone of the dataset’s annotation structure, providing a holistic view of the diverse activities and interactions within the sub-group and overall group scenarios. This level of detail sets GASG apart, making it a valuable resource for research in scene comprehension, action recognition, and group activity analysis. The annotation process is detailed in the *Appendix*.

3.2. Dataset Statistics

The accompanying pie chart in Fig. 3 b.) delves into the complexity of attributes in our dataset, revealing that “Appearance” consists of 33% of the total annotations, which is the highest, “Relationship” consists of 28%, “Interaction” consists of 17%, “Position” consists of 12% and “Situation” consists of 10% which is the least. We explore the distribution of social activity labels in Fig. 3 a.), focusing on the sizes of social groups. The chart in the figure provides a nuanced view of social group sizes in the dataset. Specifically, 75.5%, 16.6%, 5%, and 1.2% of social groups consist of one, two, three, and four members, respectively. Interestingly, only 1% of the dataset includes groups with five or more members, with the maximum observed group size being 29 members.

4. Methodology

We utilized pre-trained visual and textual backbones to extract the corresponding subject features in the video \mathbf{v} and textual features \mathbf{t} . In the input preparation section, these are h to represent the nodes and e to represent the edges. However, we denote the visual nodes as \mathbf{v} , textual nodes as \mathbf{t} and textual edges as \mathbf{t}_e in Fig. 4. We used the Graph Transformer

Layer and the Graph Transformer Layer with edge features to extract the corresponding feature representations. The former is tailored for graphs lacking explicit edge attributes, while the latter incorporates a dedicated edge feature pipeline to integrate available edge information, maintaining abstract representations at each layer.

Input Preparation Initially, we prepare input node and edge embeddings for the Graph Transformer Layer. In the context of our model, text features are employed to generate both nodes and edges, whereas vision features are exclusively utilized for generating nodes. Consider a graph \mathcal{G} with node features represented as text features $\alpha_i \in \mathbb{R}^{d_n \times 1}$ for each node i and edge features, also derived from text, denoted as $\beta_{ij} \in \mathbb{R}^{d_e \times 1}$ for edges between nodes i and j . The input node features α_i and edge features β_{ij} undergo a linear projection to be embedded into d -dimensional hidden features h_i^0 and e_{ij}^0 .

$$\hat{h}_i^0 = A^0 \alpha_i + a^0; e_{ij}^0 = B^0 \beta_{ij} + b^0, \quad (1)$$

Here, $A^0 \in \mathbb{R}^{d \times d_n}$, $B^0 \in \mathbb{R}^{d \times d_e}$, and $a^0, b^0 \in \mathbb{R}^d$ are parameters of the linear projection layers. The pre-computed node positional encodings of dimension k are linearly projected and added to the node features \hat{h}_i^0 .

$$\lambda_i^0 = C^0 \lambda_i + c^0; h_i^0 = \hat{h}_i^0 + \lambda_i^0, \quad (2)$$

Here, $C^0 \in \mathbb{R}^{d \times k}$ and $c^0 \in \mathbb{R}^d$. Notably, positional encodings are only added to the node features at the input layer and not during intermediate graph transformer layers. The detailed information about the Graph transformer layers will be presented in *Appendix*.

4.1. Hierarchical Awareness Induction

We propose enriching the vision and language branches through a hierarchy-aware attention mechanism. In line with the conventional transformer architecture, we divide modality inputs into low-level video patches and text tokens. These are recursively merged based on semantic and spatial similarities, gradually forming more semantically concentrated clusters, such as video objects and text phrases. We define hierarchy aggregation priors with the following aspects:

Tendency to merge. Patches and tokens are recursively merged into higher-level clusters that are *spatially and semantically* similar. If two nearby video patches share similar appearances, merging them is a natural step to convey the same semantic information.

Non-splittable. Once patches or tokens are merged, they will *never be split* in later layers. This constraint ensures that hierarchical information aggregation never degrades, preserving the complete process of hierarchy evolution layer by layer.

We incorporate these hierarchy aggregation priors into an attention mask C , serving as an extra inductive bias to help

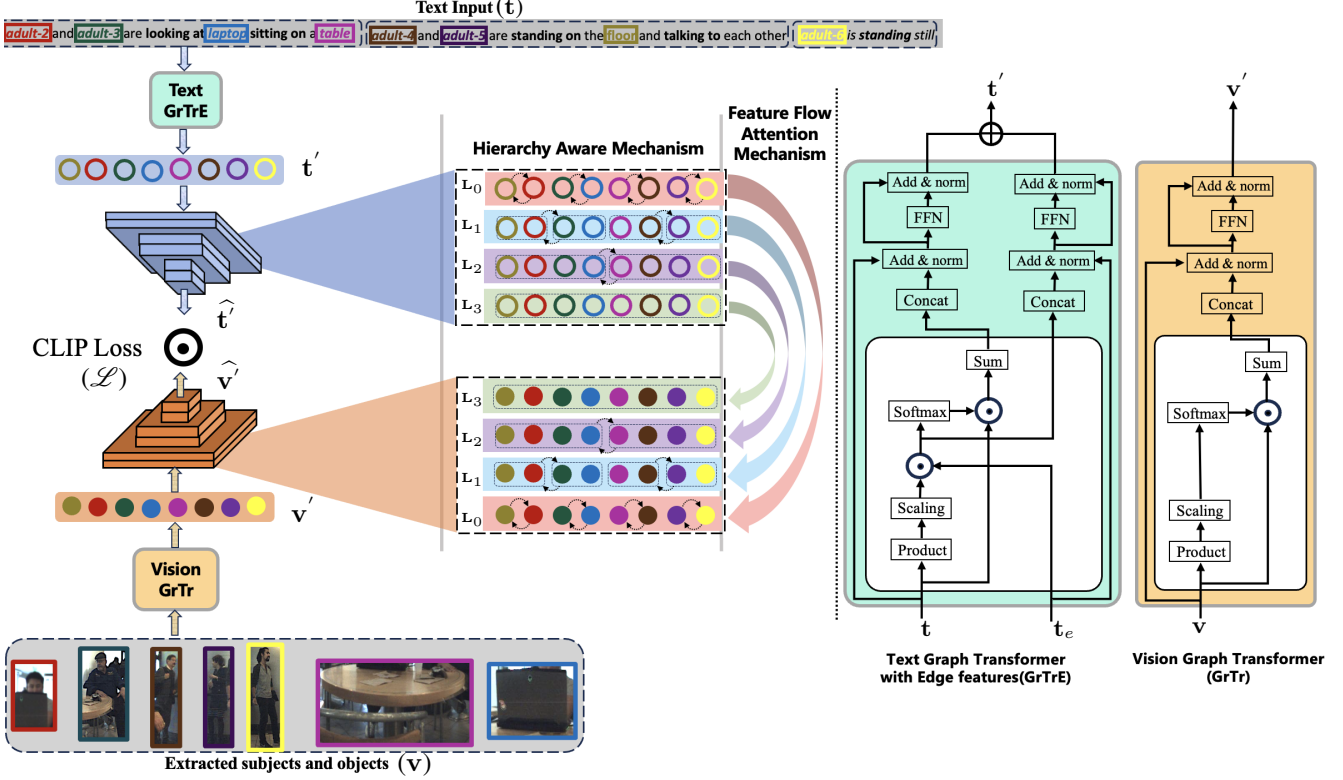


Figure 4. **Overall architecture of the proposed HAtt-Flow network.** The extracted visual and textual features are passed through their respective graph transformers to obtain corresponding node features. These nodes are passed through the hierarchy-aware-based transformer encoder models to have enriched features, including a feature flow attention mechanism to enhance cross-modality learning. Finally, we use CLIP loss to optimize the learned features. Please refer to Fig. 2 for the details of levels L_0 , L_1 , L_2 and L_3 .

the conventional attention mechanism in Transformers better explore hierarchical structures adapted to each modality format—2D grid for videos and 1D sequence for texts. Thus, the proposed hierarchy-aware attention is defined as:

$$\text{Hierarchy_Attention} = \left(C \odot \text{softmax} \left(\frac{QK^T}{\sqrt{d_h}} \right) \right) V \quad (3)$$

Note that C is shared among all heads and progressively updated bottom-up across Transformer layers. We elaborate on the formulations of the hierarchy-aware mask C for each modality as follows.

Hierarchy Induction for Language Branch

In this section, we reconsider the tree-transformer method from the perspective of the proposed hierarchy-aware attention, explaining how to impose hierarchy aggregation priors on C in three steps.

Generate neighboring attention score. The merging tendency of adjacent word tokens is described through neighboring attention scores. Two learnable key and query matrices W'_Q and W'_K transfer any adjacent word tokens (t_i, t_{i+1}) . The neighboring attention score $s_{i,i+1}$ is defined as their

inner product:

$$s_{i,i+1} = \frac{(t_i W'_Q) \cdot (t_{i+1} W'_K)}{\sigma_t} \quad (4)$$

Here, σ_t is a hyperparameter controlling the scale of the generated scores. A softmax function for each token t_i is employed to normalize its merging tendency with two neighbors:

$$p_{i,i+1}, p_{i,i-1} = \text{softmax}(s_{i,i+1}, s_{i,i-1}) \quad (5)$$

For neighbor pairs (t_i, t_{i+1}) , the neighboring affinity score $\hat{a}_{i,i+1}$ is the geometric mean of $p_{i,i+1}$ and $p_{i+1,i}$: $\hat{a}_{i,i+1} = \sqrt{p_{i,i+1} \cdot p_{i+1,i}}$. In a graph perspective, it describes the strength of edge $e_{i,i+1}$ by comparing it with edges $e_{i-1,i}$ ($p_{i,i+1}$ v.s. $p_{i,i-1}$) and $e_{i+1,i+2}$ ($p_{i+1,i}$ v.s. $p_{i+1,i+2}$).

Enforcing Non-splittable property. A higher neighboring affinity score indicates that two neighbor tokens are more closely bonded. To ensure that merged tokens will not be split, layer-wise affinity scores $a_{i,i+1}^l$ should increase as the network goes deeper, i.e., $a_{i,i+1}^l \geq a_{i,i+1}^{l-1}$ for all l . It helps gradually generate a desired hierarchy structure:

$$a_{i,i+1}^l = a_{i,i+1}^{l-1} + (1 - a_{i,i+1}^{l-1}) \hat{a}_{i,i+1}^l \quad (6)$$

Similarly, we formulate the *Hierarchy Induction for Visual Branch*, detailed in the *Appendix*.

4.2. Feature Flow Attention Mechanism

In the following representation, we use the corresponding nodes h from the respective branches of language and visual graph transformers as the queries (\mathbf{Q}), keys (\mathbf{K}) and values (\mathbf{V}).

Inspired by flow network theory, the Flow-Attention mechanism introduces a competitive mechanism for sources and an allocation mechanism for sinks, preventing the generation of trivial attention. In a flow network framework, attention is viewed as the flow of information from sources to sinks. The results (\mathbf{R}) act as endpoints receiving inbound information flow, and the values (\mathbf{V}) serve as sources providing outgoing information flow.

Flow Capacity Calculation. For a scenario with n sinks and m sources, incoming flow I_i for the i -th sink and outgoing flow O_j for the j -th source are calculated as:

$$\begin{aligned} I_i &= \phi(\mathbf{Q}_i) \sum_{j=1}^m \phi(\mathbf{K}_j)^\top, \\ O_j &= \phi(\mathbf{K}_j) \sum_{i=1}^n \phi(\mathbf{Q}_i)^\top, \end{aligned} \quad (7)$$

where $\phi(\cdot)$ is a non-negative function.

Flow Conservation. We establish the preservation of incoming flow capacity for each sink, maintaining the default value at 1, effectively "locking in" the information forwarded to the next layer. This conservation strategy ensures that the outgoing flow capacities of sources engage in competition, with their collective sum strictly constrained to 1. Likewise, by conserving the outgoing flow capacity for each source at the default value of 1, essentially "fixing" the information acquired from the previous layer, the conservation of incoming and outgoing flow capacities is enforced by normalizing operations:

$$\frac{\phi(\mathbf{K})}{\mathbf{O}}, \frac{\phi(\mathbf{Q})}{\mathbf{I}}, \quad (8)$$

In this context, the ratio denotes element-wise division, with $\frac{\phi(\mathbf{K})}{\mathbf{O}}$ dedicated to source conservation and $\frac{\phi(\mathbf{Q})}{\mathbf{I}}$ assigned for sink conservation.

This normalization process ensures the preservation of flow capacity for each source and sink token, as evidenced by the following equations:

$$\begin{aligned} \text{source-}j: \quad & \frac{\phi(\mathbf{K}_j)^\top}{O_j} \sum_{i=1}^n \phi(\mathbf{Q}_i) = \frac{\sum_{i=1}^n \phi(\mathbf{Q}_i) \phi(\mathbf{K}_j)^\top}{O_j} = 1 \\ \text{sink-}i: \quad & \frac{\phi(\mathbf{Q}_i)^\top}{I_i} \sum_{j=1}^m \phi(\mathbf{K}_j) = \frac{\sum_{j=1}^m \phi(\mathbf{K}_j) \phi(\mathbf{Q}_i)^\top}{I_i} = 1 \end{aligned} \quad (9)$$

These equations replicate the same computations as Eq. (7). The initial equation concerns the outgoing flow capacity of the j -th source after the normalization process $\frac{\phi(\mathbf{K})}{\mathbf{O}}$. In contrast, the second equation corresponds to the incoming flow capacity of the i -th sink after the normalization process $\frac{\phi(\mathbf{Q})}{\mathbf{I}}$. In both instances, the capacities are identical to the default value of 1.

The conserved incoming flow $\hat{\mathbf{I}}$ and outgoing flow $\hat{\mathbf{O}}$ are represented as:

$$\begin{aligned} \hat{\mathbf{I}} &= \phi(\mathbf{Q}) \sum_{j=1}^m \frac{\phi(\mathbf{K}_j)^\top}{O_j}, \\ \hat{\mathbf{O}} &= \phi(\mathbf{K}) \sum_{i=1}^n \frac{\phi(\mathbf{Q}_i)^\top}{I_i} \end{aligned} \quad (10)$$

Flow-Attention Mechanism. We introduce the Flow-Attention mechanism, leveraging competition induced by incoming flow conservation for sinks. In $\hat{\mathbf{O}}$, sources compete while maintaining a fixed flow capacity sum, revealing source significance. $\hat{\mathbf{I}}$ represents sink information when source outgoing capacity is 1, reflecting aggregated information allocation to each sink. The Flow-Attention equations are:

$$\begin{aligned} \text{Competition: } \hat{\mathbf{V}} &= \text{Softmax}(\hat{\mathbf{O}}) \odot \mathbf{V} \\ \text{Aggregation: } \mathbf{A} &= \frac{\phi(\mathbf{Q})}{\mathbf{I}} (\phi(\mathbf{K})^\top \hat{\mathbf{V}}) \\ \text{Allocation: } \mathbf{R} &= \text{Sigmoid}(\hat{\mathbf{I}}) \odot \mathbf{A}. \end{aligned} \quad (11)$$

In the "Competition" stage, $\hat{\mathbf{V}}$ is determined through the application of the Softmax function to $\hat{\mathbf{O}}$, followed by element-wise multiplication with \mathbf{V} . The "Aggregation" step, denoted as \mathbf{A} , is computed using the presented equation. Lastly, the "Allocation" phase calculates \mathbf{R} by employing the Sigmoid function on $\hat{\mathbf{I}}$, which is then element-wise multiplied with \mathbf{A} .

4.3. Training Loss

To adapt the contrastive pretraining objective for video and text features in the HAtt-Flow architecture, the objective function can be expressed as follows:

$$\begin{aligned} \mathcal{L} &= -\frac{1}{M} \sum_i \log \frac{\exp(\mathbf{v}_i^\top \mathbf{u}_i / \tau)}{\sum_{j=1}^M \exp(\mathbf{v}_i^\top \mathbf{u}_j / \tau)} \\ &\quad -\frac{1}{M} \sum_i \log \frac{\exp(\mathbf{u}_i^\top \mathbf{v}_i / \tau)}{\sum_{j=1}^M \exp(\mathbf{u}_i^\top \mathbf{v}_j / \tau)} \end{aligned} \quad (12)$$

Here, \mathbf{v} and \mathbf{u} represent the video and text feature vectors, τ is the learnable temperature parameter, and M is the total number of video-text pairs, i.e., the total number of labels.

5. Experimental Results

5.1. Experiment Settings

Dataset Details. Our dataset adopts a division strategy from JRDB [41], where videos are segregated at the sequence level, ensuring the entirety of a video sequence is allocated to a specific split. The 54 video sequences are distributed, with 20 for training, 7 for validation, and 27 for testing. To align with the evaluation practices of analogous datasets, our evaluation is centered on keyframes sampled at one-second intervals, resulting in 1419 training samples, 404 validation samples, and 1802 test samples.

Implementation Details. Our framework, implemented in PyTorch, undergoes training on a machine featuring four NVIDIA Quadro RTX 6000 GPUs. During training, we adopt a batch size of 2 and leverage the Adam Optimizer, commencing the training process with an initial learning rate set at 0.0001.

Evaluation Metrics. We evaluate the model on two tasks: 1.) Predicate Classification (PredCls) and 2.) Video Scene Graph Generation (VSGG). The Video Scene Graph Generation (VSGG) task aims to generate descriptive triplets for an input video. Each triplet, denoted as $(r_i, t_1, t_2, o_s, m_s^{(t_1, t_2)}, o_o, m_o^{(t_1, t_2)})$, consists of a relation r_i occurring between time points t_1 and t_2 , connecting a subject o_s (class category) with mask tube $m_s^{(t_1, t_2)}$, and an object o_o with mask tube $m_o^{(t_1, t_2)}$. Evaluation metrics for PredCls and VSGG adhere to Scene Graph Generation (SGG) standards, utilizing Recall@K (R@K) and mean Recall@K (mR@K). Successful recall for a ground-truth triplet $(\hat{o}_s, \hat{m}_s^{(\hat{t}_1, \hat{t}_2)}, \hat{o}_o, \hat{m}_o^{(\hat{t}_1, \hat{t}_2)}, \hat{r}_i^{(\hat{t}_1, \hat{t}_2)})$ requires accurate category labels and IOU volumes between predicted and ground-truth mask tubes above 0.5. The soft recall is recorded when these criteria are met, considering the time IOU between predicted and ground-truth intervals.

Table 2. Comparison with SOTA methods on **GASG dataset**.

Method	Modality (X)	R/mR@20		R/mR@50		R/mR@100	
		PredCls	VSGG	PredCls	VSGG	PredCls	VSGG
IMP [60]	Image	31.9/9.55	16.5/6.52	36.8/10.9	18.2/7.05	38.9/11.6	18.6/7.23
	Video	-	-	-	-	-	-
MOTIFS [69]	Image	44.9/20.2	20.0/9.10	50.4/20.1	21.7/9.57	52.4/22.9	22.0/9.67
	Video	-	-	-	-	-	-
VCTree [52]	Image	45.3/20.7	20.6/9.70	50.8/22.6	22.1/10.2	52.7/23.3	22.5/10.2
	Video	-	-	-	-	-	-
GPSNet [38]	Image	31.5/13.2	17.8/2.03	39.9/16.4	19.6/7.49	44.7/18.3	20.1/7.67
	Video	-	-	-	-	-	-
PSG [64]	Image	-	31.4/16.2	-	32.9/21.5	-	36.1/22.7
	Video	-	-	-	-	-	-
PVSG [65]	Image	-	38.3/18.1	-	41.7/20.8	-	43.2/23.7
	Video	-	13.6/10.2	-	19.2/11.1	-	26.5/14.7
Ours	Image	57.4/35.2	42.2/21.4	60.2/36.1	44.5/23.1	63.7/39.5	48.1/26.9
	Video	27.1/14.3	11.2/9.1	29.5/17.71	19.6/12.3	41.7/24.2	30.2/18.1

5.2. Comparison with State-of-the-art

We present our comparisons with state-of-the-art methods in Tab. 2 and Tab. 3 for our dataset and PSG dataset. In direct comparison with the methods above, the HAtt-Flow model

Table 3. Comparison with SOTA methods on **PSG dataset**.

Methods	R/mR@20		R/mR@50		R/mR@100	
	PredCls	VSGG	PredCls	VSGG	PredCls	VSGG
IMP [60]	30.5/8.97	17.9/7.35	35.9/10.5	19.5/7.88	38.3/11.3	20.1/8.02
MOTIFS [69]	45.1/19.9	20.9/9.60	50.5/21.5	22.5/10.1	52.5/22.2	23.1/10.3
VCTree [52]	45.9/21.4	21.7/9.68	51.2/23.1	23.3/10.2	53.1/23.8	23.7/10.3
GPSNet [38]	38.8/17.1	18.4/6.52	46.6/20.2	20.0/6.97	50.0/21.3	20.6/7.2
PSG [64]	-	28.2/15.4	-	32.1/20.3	-	35.3/21.5
Ours	52.4/25.6	32.9/18.4	56.1/28.3	35.3/21.6	62.7/32.12	41.34/23.1

exhibits a notable performance advantage, establishing itself as the current state-of-the-art. This superiority is attributed to its proficiency in capturing intricate social activities among subjects across spatial and temporal dimensions. On the GASG dataset, our proposed method outperforms existing SGG methods by a significant margin on all metrics except for the R/mR@20 of the VSGG task. On the PSG dataset, it is evident that the proposed method dominated the other methods to demonstrate state-of-the-art performance.

5.3. Ablation Study

Flow Attention Direction. We introduced a novel flow attention mechanism between the hierarchical transformers handling text and vision. To explore the impact of the flow direction between these networks, we conducted experiments as detailed in Tab. 4. Our findings validate that optimal results are achieved when attention flows from the text to the vision transformer. Conversely, performance declines in the opposite direction, notably when no attention flows. This observation suggests that the cross-attention mechanism enhances the model’s contextual learning capacity primarily when the flow is from text to vision because text often provides high-level semantic information and context that can guide the understanding of visual content.

Importance of Hierarchy awareness. We incorporated hierarchy awareness into the transformer framework to bolster the model’s scene graph generation capabilities. Experimental results, detailed in Tab. 5, affirm that hierarchical awareness optimally enhances scene graph generation. Conversely, performance declines in the absence of this design. It is likely because when the model is aware of the hierarchy during the generation of video scene graphs, it accurately predicts all relevant nodes and their relationships (edges).

Attributes Analysis. In Tab. 6, we evaluate the impact of different attributes in the dataset on the model’s performance in scene graph generation. Our findings affirm that including all attributes results in optimal scene graph generation. Conversely, the performance exhibits a decline when we consider individual attribute at a time. We can clearly observe the performance is proportional to the attribute distribution as shown in Fig. 3 b.) i.e., more the number of attributes better the performance. It underscores the significance of leveraging all attributes, indicating that they collectively enhance the model’s capacity to grasp intricate contexts, enabling accurate scene graph generation.

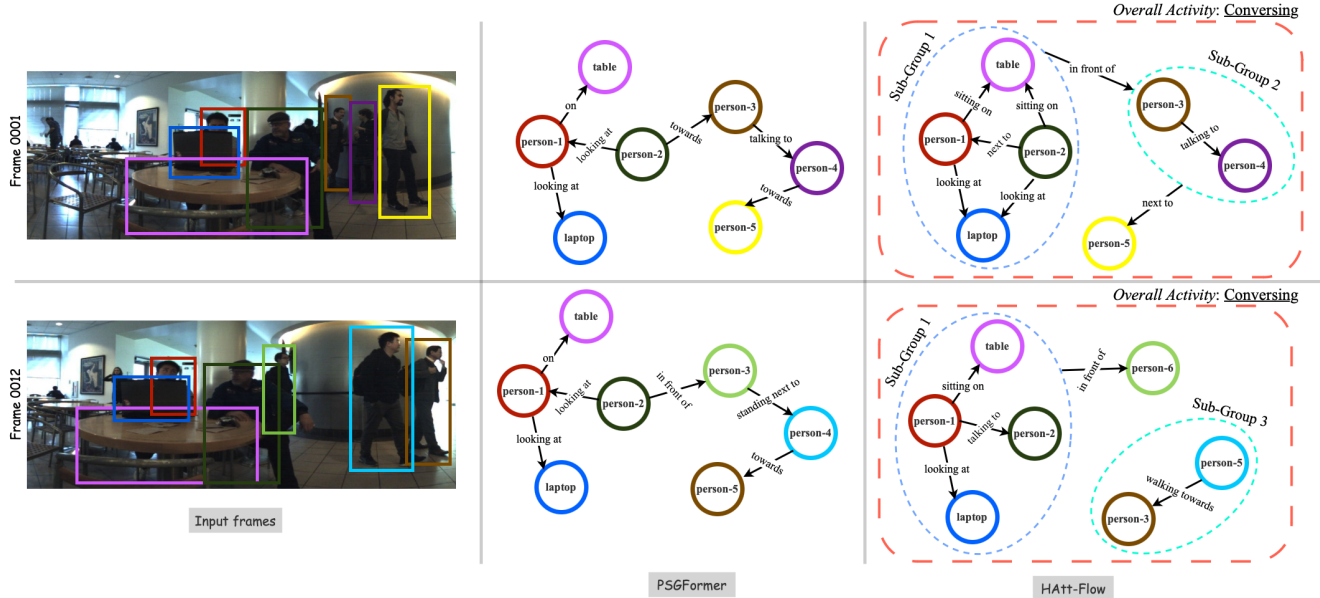


Figure 5. **The visualization of the scene graphs generated by PSGFormer [64] and Ours.** We can observe that [64] could only detect the subjects but not accurate groups and their interactions. In contrast, the HAtt-Flow is accurate in graph generation and overall group activity prediction. **Best viewed in color and zoomed.**

Table 4. Ablation Study for **Flow Attention direction.**

Flow Attention Direction	Modality (X)	R/mR@20		R/mR@50		R/mR@100	
		PredCls	VSGG	PredCls	VSGG	PredCls	VSGG
T → X	Image	32.1/17.4	18.3/9.2	37.15/19.2	21.4/10.5	41.6/21.8	23.5/14.7
	Video	10.2/5.3	4.7/2.4	12.7/7.5	7.1/4.2	16.2/10.8	9.8/7.3
X → T	Image	45.3/23.84	20.4/10.8	48.1/25.6	23.5/12.4	52.8/27.3	29.2/16.1
	Video	15.4/7.1	7.2/4.7	18.3/9.4	9.7/6.2	24.7/12.1	14.1/9.4
T → X	Image	57.4/35.2	42.2/21.4	60.2/36.1	44.5/23.1	63.7/39.5	48.1/26.9
	Video	27.1/14.3	11.2/9.1	29.5/17.71	19.6/12.3	41.7/24.2	30.2/18.1

Table 5. Ablation Study for **Hierarchy Awareness.**

Hierarchy Awareness	Modality (X)	R/mR@20		R/mR@50		R/mR@100	
		PredCls	VSGG	PredCls	VSGG	PredCls	VSGG
✗	Image	46.1/22.3	23.7/12.5	47.2/24.1	24.5/13.4	52.6/28.3	29.8/16.1
	Video	17.5/11.3	10.4/8.7	22.1/14.1	14.1/9.61	27.4/15.2	25.7/16.3
✓	Image	57.4/35.2	42.2/21.4	60.2/36.1	44.5/23.1	63.7/39.5	48.1/26.9
	Video	27.1/14.3	11.2/9.1	29.5/17.71	19.6/12.3	41.7/24.2	30.2/18.1

Table 6. Ablation study for **Attributes** in our dataset.

Attributes	R/mR@20		R/mR@50		R/mR@100	
	PredCls	VSGG	PredCls	VSGG	PredCls	VSGG
Appearance	14.5/2.3	1.4/0.3	17.2/6.1	2.3/0.5	21.1/9.1	7.8/2.1
Relationship	13.2/1.8	1.3/0.5	16.4/5.2	2.1/0.4	20.8/8.7	7.5/2.4
Interaction	11.4/1.4	0.9/0.4	14.7/4.1	1.7/0.7	17.7/6.4	6.2/1.6
Position	8.1/0.7	1.5/0.51	10.6/3.7	1.4/0.4	14.2/4.7	4.1/0.9
Situation	5.7/0.2	0.7/0.2	7.2/1.7	0.9/0.3	10.1/2.8	2.8/0.4
All together	27.1/14.3	11.2/9.1	29.5/17.71	19.6/12.3	41.7/24.2	30.2/18.1

6. Qualitative Analysis

To gain deeper insights into the performance of HAtt-Flow, we employ visualization to illustrate its scene graph generation predictions using our dataset. As depicted in Fig. 5, our model substantially improves overall scene graph generation compared to PSGFormer. The effectiveness of our hierarchy-

aware attention-flow mechanism contributes significantly to this enhancement, providing our model with superior context modeling capabilities for visual representations guided by textual inputs.

7. Conclusions

In this work, we introduced a pioneering dataset designed with nuanced attributes, specifically tailored to enhance the scene graph generation task within the context of group activities. Our contributions extend to advancing predictive video scene understanding, propelled by the introduction of the Flow-Attention and a paradigm shift in attention mechanisms through hierarchy awareness. Through rigorous experimentation, we demonstrate the efficacy of our approach, showcasing significant improvements over existing methods. **Limitations:** This work presents a novel Flow-Attention mechanism inspired by flow network theory, which introduces competition and allocation principles for attention modeling, preventing trivial attention patterns. While offering promising advancements, this approach presents some limitations. Firstly, implementing Flow-Attention entails heightened computational demands, potentially restricting its use in resource-constrained settings. Additionally, the model’s performance is notably sensitive to the quality and quantity of training data, necessitating substantial data resources for optimal results. Balancing these computational and data requirements is essential to maximize the practicality and effectiveness of the proposed Flow-Attention mechanism in real-world applications.

References

- [1] Mohamed R Amer and Sinisa Todorovic. Sum product networks for activity recognition. 38(4):800–813, 2015. 2
- [2] Mohamed R Amer, Dan Xie, Mingtian Zhao, Sinisa Todorovic, and Song-Chun Zhu. Cost-sensitive top-down/bottom-up inference for multiscale activity recognition. In *ECCV*, pages 187–200. Springer, 2012.
- [3] Mohamed R Amer, Sinisa Todorovic, Alan Fern, and Song-Chun Zhu. Monte carlo tree search for scheduling activity recognition. In *ICCV*, pages 1353–1360, 2013.
- [4] Mohamed Rabie Amer, Peng Lei, and Sinisa Todorovic. Hrf: Hierarchical random field for collective activity recognition in videos. In *ECCV*, pages 572–585. Springer, 2014. 2
- [5] Timur Bagautdinov, Alexandre Alahi, François Fleuret, Pascal Fua, and Silvio Savarese. Social scene understanding: End-to-end multi-person action localization and collective activity recognition. In *CVPR*, pages 4315–4324, 2017. 3
- [6] Fabian Caba Heilbron, Victor Escorcia, Bernard Ghanem, and Juan Carlos Niebles. Activitynet: A large-scale video benchmark for human activity understanding. In *Proceedings of the IEEE conference on computer vision and pattern recognition*, pages 961–970, 2015. 2
- [7] Yu-Wei Chao, Yunfan Liu, Xieyang Liu, Huayi Zeng, and Jia Deng. Learning to detect human-object interactions. In *Proceedings of the IEEE Winter Conference on Applications of Computer Vision (WACV)*, 2018. 2, 3
- [8] Tianshui Chen, Weihao Yu, Riquan Chen, and Liang Lin. Knowledge-embedded routing network for scene graph generation. In *CVPR*, 2019. 3
- [9] Bo Dai, Yuqi Zhang, and Dahua Lin. Detecting visual relationships with deep relational networks. In *CVPR*, 2017. 3
- [10] Zhiwei Deng, Arash Vahdat, Hexiang Hu, and Greg Mori. Structure inference machines: Recurrent neural networks for analyzing relations in group activity recognition. In *CVPR*, pages 4772–4781, 2016. 3
- [11] Alakh Desai, Tz-Ying Wu, Subarna Tripathi, and Nuno Vasconcelos. Learning of visual relations: The devil is in the tails. In *ICCV*, 2021. 2
- [12] Linsen Dong, Guanyu Gao, Xinyi Zhang, Liangyu Chen, and Yonggang Wen. Baconian: A unified open-source framework for model-based reinforcement learning. *arXiv preprint arXiv:1904.10762*, 2019. 3
- [13] Chen Gao, Jiarui Xu, Yuliang Zou, and Jia-Bin Huang. Drg: Dual relation graph for human-object interaction detection. In *ECCV*, 2020. 2, 3
- [14] Kirill Gavrilyuk, Ryan Sanford, Mehrsan Javan, and Cees GM Snoek. Actor-transformers for group activity recognition. In *CVPR*, pages 839–848, 2020. 3
- [15] Georgia Gkioxari, Ross Girshick, Piotr Dollár, and Kaiming He. Detecting and recognizing human-object interactions. In *CVPR*, 2018. 2, 3
- [16] Jiuxiang Gu, Handong Zhao, Zhe Lin, Sheng Li, Jianfei Cai, and Mingyang Ling. Scene graph generation with external knowledge and image reconstruction. In *CVPR*, 2019. 3
- [17] Saurabh Gupta and Jitendra Malik. Visual semantic role labeling. *arXiv preprint arXiv:1505.04474*, 2015. 2
- [18] Mingfei Han, David Junhao Zhang, Yali Wang, Rui Yan, Lina Yao, Xiaojun Chang, and Yu Qiao. Dual-ai: Dual-path actor interaction learning for group activity recognition. In *Proceedings of the IEEE/CVF Conference on Computer Vision and Pattern Recognition*, pages 2990–2999, 2022. 3
- [19] Zhi Hou, Xiaojiang Peng, Yu Qiao, and Dacheng Tao. Visual compositional learning for human-object interaction detection. In *ECCV*, 2020. 2, 3
- [20] Zhi Hou, Baosheng Yu, Yu Qiao, Xiaojiang Peng, and Dacheng Tao. Affordance transfer learning for human-object interaction detection. In *CVPR*, 2021. 2, 3
- [21] Zih-Siou Hung, Arun Mallya, and Svetlana Lazebnik. Contextual translation embedding for visual relationship detection and scene graph generation. *IEEE TPAMI*, 2020. 2
- [22] Mostafa S Ibrahim and Greg Mori. Hierarchical relational networks for group activity recognition and retrieval. In *ECCV*, pages 721–736, 2018. 3
- [23] Mostafa S Ibrahim, Srikanth Muralidharan, Zhiwei Deng, Arash Vahdat, and Greg Mori. A hierarchical deep temporal model for group activity recognition. In *CVPR*, pages 1971–1980, 2016. 3
- [24] Justin Johnson, Ranjay Krishna, Michael Stark, Li-Jia Li, David Shamma, Michael Bernstein, and Li Fei-Fei. Image retrieval using scene graphs. In *CVPR*, 2015. 3
- [25] Keizo Kato, Yin Li, and Abhinav Gupta. Compositional learning for human object interaction. In *ECCV*, 2018. 2, 3
- [26] Siddhesh Khandelwal, Mohammed Suhail, and Leonid Sigal. Segmentation-grounded scene graph generation. In *ICCV*, 2021. 2, 3
- [27] Bumsoo Kim, Taeho Choi, Jaewoo Kang, and Hyunwoo J Kim. Uniondet: Union-level detector towards real-time human-object interaction detection. In *ECCV*, 2020. 2, 3
- [28] Bumsoo Kim, Junhyun Lee, Jaewoo Kang, Eun-Sol Kim, and Hyunwoo J Kim. Hotr: End-to-end human-object interaction detection with transformers. In *CVPR*, 2021. 2
- [29] Alexander Kolesnikov, Alina Kuznetsova, Christoph Lampert, and Vittorio Ferrari. Detecting visual relationships using box attention. In *CVPRW*, 2019. 3
- [30] Tian Lan, Yang Wang, Weilong Yang, Stephen N Robinovitch, and Greg Mori. Discriminative latent models for recognizing contextual group activities. 34(8):1549–1562, 2011. 2
- [31] Tian Lan, Leonid Sigal, and Greg Mori. Social roles in hierarchical models for human activity recognition. In *CVPR*, pages 1354–1361. IEEE, 2012. 2
- [32] Xin Li and Mooi Choo Chuah. Sbgar: Semantics based group activity recognition. In *ICCV*, pages 2876–2885, 2017. 3
- [33] Xinghang Li, Di Guo, Huaping Liu, and Fuchun Sun. Embodied semantic scene graph generation. In *Conference on Robot Learning*, pages 1585–1594. PMLR, 2022. 3
- [34] Yikang Li, Wanli Ouyang, Bolei Zhou, Jianping Shi, Chao Zhang, and Xiaogang Wang. Factorizable net: an efficient subgraph-based framework for scene graph generation. In *ECCV*, 2018. 3
- [35] Yong-Lu Li, Siyuan Zhou, Xijie Huang, Liang Xu, Ze Ma, Hao-Shu Fang, Yanfeng Wang, and Cewu Lu. Transferable interactiveness knowledge for human-object interaction detection. In *CVPR*, 2019. 2, 3

- [36] Yong-Lu Li, Xinpeng Liu, Han Lu, Shiyi Wang, Junqi Liu, Jiefeng Li, and Cewu Lu. Detailed 2d-3d joint representation for human-object interaction. In *CVPR*, 2020. 2, 3
- [37] Yuanzhi Liang, Yalong Bai, Wei Zhang, Xueming Qian, Li Zhu, and Tao Mei. Vrr-vg: Refocusing visually-relevant relationships. In *ICCV*, 2019. 2
- [38] Xin Lin, Changxing Ding, Jinqian Zeng, and Dacheng Tao. Gps-net: Graph property sensing network for scene graph generation. In *CVPR*, 2020. 3, 7
- [39] Yang Liu, Qingchao Chen, and Andrew Zisserman. Amplifying key cues for human-object-interaction detection. In *ECCV*, 2020. 2, 3
- [40] Cewu Lu, Ranjay Krishna, Michael Bernstein, and Li Fei-Fei. Visual relationship detection with language priors. In *Proceedings of the European Conference on Computer Vision (ECCV)*, pages 852–869, 2016. 3
- [41] Roberto Martin-Martin, Mihir Patel, Hamid Rezafofighi, Abhijeet Sheno, JunYoung Gwak, Eric Frankel, Amir Sadeghian, and Silvio Savarese. Jrdb: A dataset and benchmark of ego-centric robot visual perception of humans in built environments. *IEEE transactions on pattern analysis and machine intelligence*, 2021. 7
- [42] Yingwei Pan, Ting Yao, Houqiang Li, and Tao Mei. Video captioning with transferred semantic attributes. In *Proceedings of the IEEE conference on computer vision and pattern recognition*, pages 6504–6512, 2017. 2
- [43] Mengshi Qi, Jie Qin, Annan Li, Yunhong Wang, Jiebo Luo, and Luc Van Gool. stagnet: An attentive semantic rnn for group activity recognition. In *ECCV*, pages 101–117, 2018. 3
- [44] Mengshi Qi, Weijian Li, Zhengyuan Yang, Yunhong Wang, and Jiebo Luo. Attentive relational networks for mapping images to scene graphs. In *CVPR*, 2019. 3
- [45] Xindi Shang, Tongwei Ren, Jingfan Guo, Hanwang Zhang, and Tat-Seng Chua. Video visual relation detection. In *Proceedings of the 25th ACM international conference on Multimedia*, pages 1300–1308, 2017. 3
- [46] Tianmin Shu, Dan Xie, Brandon Rothrock, Sinisa Todorovic, and Song Chun Zhu. Joint inference of groups, events and human roles in aerial videos. In *CVPR*, pages 4576–4584, 2015. 2
- [47] Xiangbo Shu, Jinhui Tang, Guojun Qi, Wei Liu, and Jian Yang. Hierarchical long short-term concurrent memory for human interaction recognition. 2019. 3
- [48] Mohammed Suhail, Abhay Mittal, Behjat Siddiquie, Chris Broaddus, Jayan Eledath, Gerard Medioni, and Leonid Sigal. Energy-based learning for scene graph generation. In *CVPR*, 2021. 3
- [49] Masato Tamura, Hiroki Ohashi, and Tomoaki Yoshinaga. Qpic: Query-based pairwise human-object interaction detection with image-wide contextual information. In *CVPR*, 2021. 2, 3
- [50] Masato Tamura, Rahul Vishwakarma, and Ravigopal Venelakanti. Hunting group clues with transformers for social group activity recognition. In *Computer Vision–ECCV 2022: 17th European Conference, Tel Aviv, Israel, October 23–27, 2022, Proceedings, Part IV*, pages 19–35. Springer, 2022. 3
- [51] Kaihua Tang, Hanwang Zhang, Baoyuan Wu, Wenhan Luo, and Wei Liu. Learning to compose dynamic tree structures for visual contexts. In *CVPR*, 2019. 3
- [52] Kaihua Tang, Hanwang Zhang, Baoyuan Wu, Wenhan Luo, and Wei Liu. Learning to compose dynamic tree structures for visual contexts. In *Proceedings of the IEEE/CVF conference on computer vision and pattern recognition*, pages 6619–6628, 2019. 7
- [53] Kaihua Tang, Yulei Niu, Jianqiang Huang, Jiabin Shi, and Hanwang Zhang. Unbiased scene graph generation from biased training. In *CVPR*, 2020. 2
- [54] Yao Teng, Limin Wang, Zhifeng Li, and Gangshan Wu. Target adaptive context aggregation for video scene graph generation. In *Proceedings of the IEEE/CVF International Conference on Computer Vision*, pages 13688–13697, 2021. 3
- [55] Minsi Wang, Bingbing Ni, and Xiaokang Yang. Recurrent modeling of interaction context for collective activity recognition. In *CVPR*, pages 3048–3056, 2017. 3
- [56] Suchen Wang, Yueqi Duan, Henghui Ding, Yap-Peng Tan, Kim-Hui Yap, and Junsong Yuan. Learning transferable human-object interaction detector with natural language supervision. In *CVPR*, 2022. 2, 3
- [57] Tiancai Wang, Rao Muhammad Anwer, Muhammad Haris Khan, Fahad Shahbaz Khan, Yanwei Pang, Ling Shao, and Jorma Laaksonen. Deep contextual attention for human-object interaction detection. In *ICCV*, 2019.
- [58] Tiancai Wang, Tong Yang, Martin Danelljan, Fahad Shahbaz Khan, Xiangyu Zhang, and Jian Sun. Learning human-object interaction detection using interaction points. In *CVPR*, 2020. 2, 3
- [59] Zhenhua Wang, Qinfeng Shi, Chunhua Shen, and Anton Van Den Hengel. Bilinear programming for human activity recognition with unknown mrf graphs. In *CVPR*, pages 1690–1697, 2013. 2
- [60] Danfei Xu, Yuke Zhu, Christopher B Choy, and Li Fei-Fei. Scene graph generation by iterative message passing. In *CVPR*, 2017. 3, 7
- [61] Jun Xu, Tao Mei, Ting Yao, and Yong Rui. Msr-vtt: A large video description dataset for bridging video and language. In *Proceedings of the IEEE conference on computer vision and pattern recognition*, pages 5288–5296, 2016. 2
- [62] Rui Yan, Jinhui Tang, Xiangbo Shu, Zechao Li, and Qi Tian. Participation-contributed temporal dynamic model for group activity recognition. In *Proceedings of the 26th ACM international conference on Multimedia*, pages 1292–1300, 2018. 3
- [63] Jianwei Yang, Jiasen Lu, Stefan Lee, Dhruv Batra, and Devi Parikh. Graph r-cnn for scene graph generation. In *ECCV*, 2018. 3
- [64] Jingkan Yang, Yi Zhe Ang, Zujin Guo, Kaiyang Zhou, Wayne Zhang, and Ziwei Liu. Panoptic scene graph generation. In *European Conference on Computer Vision*, pages 178–196. Springer, 2022. 2, 7, 8
- [65] Jingkan Yang, Wenxuan Peng, Xiangtai Li, Zujin Guo, Liangyu Chen, Bo Li, Zheng Ma, Kaiyang Zhou, Wayne Zhang, Chen Change Loy, et al. Panoptic video scene graph generation. In *Proceedings of the IEEE/CVF Conference*

- on *Computer Vision and Pattern Recognition*, pages 18675–18685, 2023. 2, 3, 7
- [66] Keren Ye and Adriana Kovashka. Linguistic structures as weak supervision for visual scene graph generation. In *CVPR*, 2021. 3
 - [67] Alireza Zareian, Svebor Karaman, and Shih-Fu Chang. Bridging knowledge graphs to generate scene graphs. In *ECCV*, 2020.
 - [68] Alireza Zareian, Zhecan Wang, Haoxuan You, and Shih-Fu Chang. Learning visual commonsense for robust scene graph generation. In *ECCV*, 2020. 3
 - [69] Rowan Zellers, Mark Yatskar, Sam Thomson, and Yejin Choi. Neural motifs: Scene graph parsing with global context. In *CVPR*, 2018. 3, 7
 - [70] Aixi Zhang, Yue Liao, Si Liu, Miao Lu, Yongliang Wang, Chen Gao, and Xiaobo Li. Mining the benefits of two-stage and one-stage hoi detection. *NeurIPS*, 2021. 2, 3
 - [71] Frederic Z Zhang, Dylan Campbell, and Stephen Gould. Efficient two-stage detection of human-object interactions with a novel unary-pairwise transformer. In *CVPR*, 2022. 2, 3
 - [72] Hanwang Zhang, Zawlin Kyaw, Shih-Fu Chang, and Tat-Seng Chua. Visual translation embedding network for visual relation detection. In *CVPR*, 2017. 2
 - [73] Ji Zhang, Mohamed Elhoseiny, Scott Cohen, Walter Chang, and Ahmed Elgammal. Relationship proposal networks. In *CVPR*, 2017. 3
 - [74] Yiwu Zhong, Jing Shi, Jianwei Yang, Chenliang Xu, and Yin Li. Learning to generate scene graph from natural language supervision. In *ICCV*, 2021. 3
 - [75] Tianfei Zhou, Wenguan Wang, Siyuan Qi, Haibin Ling, and Jianbing Shen. Cascaded human-object interaction recognition. In *CVPR*, 2020. 2, 3
 - [76] Cheng Zou, Bohan Wang, Yue Hu, Junqi Liu, Qian Wu, Yu Zhao, Boxun Li, Chenguang Zhang, Chi Zhang, Yichen Wei, et al. End-to-end human object interaction detection with hoi transformer. In *CVPR*, 2021. 2